

Momentum distribution of itinerant electrons in the one-dimensional Falicov-Kimball model

Pavol Farkašovský

Institute of Experimental Physics, Slovak Academy of Sciences
Watsonova 47, 043 53 Košice, Slovakia

Abstract

The momentum distribution n_k of itinerant electrons in the one-dimensional Falicov-Kimball model is calculated for various ground-state phases. In particular, we examine the periodic phases with period two, three and four (that are ground-states for all Coulomb interactions) as well as the phase separated states (that are ground states for small Coulomb interactions). For all periodic phases examined the momentum distribution is a smooth function of k with no sign of any discontinuity or singular behavior at the Fermi surface $k = k_F$. An unusual behavior of n_k (a local maximum) is found at $k = 3k_F$ for electron concentrations outside half-filling. For the phase separated ground states the momentum distribution n_k exhibits discontinuity at $k = k_0 < k_F$. This behavior is interpreted in terms of a Fermi liquid.

PACS nrs.: 71.27.+a, 71.28.+d, 71.30.+h

Keywords: Falicov-Kimball model, momentum distribution, Fermi liquid, Luttinger liquid

1 Introduction

Since its introduction in 1969 the Falicov-Kimball model [1] has become an important standard model for a description of correlated fermions on the lattice. The model describes a two-band system of localized f electrons and itinerant d electrons with the short-ranged f - d Coulomb interaction U . The Hamiltonian is

$$H = \sum_{ij} t_{ij} d_i^+ d_j + U \sum_i f_i^+ f_i d_i^+ d_i + E_f \sum_i f_i^+ f_i, \quad (1)$$

where f_i^+ , f_i are the creation and annihilation operators for an electron in the localized state at lattice site i with binding energy E_f and d_i^+ , d_i are the creation and annihilation operators for an electron in the conduction band. The conduction band is generated by the hopping matrix elements t_{ij} , which describe intersite transitions between the sites i and j (as usually, we assume that $t_{ij} = -t$ if i and j are nearest neighbors and $t_{ij} = 0$ otherwise, and all energies are measured in units of t).

The model has been used in the literature to study a great variety of many-body effects in metals, of which valence and metal-insulator transitions, charge-density waves and electronic ferroelectricity are the most common examples [2, 3]. It has been applied to a variety of lattices, one [4, 5], two [6, 7, 8], three [9], and infinite dimensional [10], and occasionally to small clusters [11, 12, 13]. Exact results are available in very few instances [10, 14, 15, 16] and general theorems have been proved for special cases [7]. In spite of the existence of an analytic solution in $d = \infty$ dimension [10, 17] and an impressive research activity in the past, the properties of this seemingly simple model are far from being understood. Indeed, while the ground-state properties of the f -electron subsystem has been satisfactory explained, only a few exact results are known concerning the ground-state correlations of the itinerant electrons [18]. Even, some important quantities such as a momentum distribution of itinerant electrons has not been explored yet. The first attempt to describe ground-

state correlations of itinerant electrons has been performed recently by Jedrzejewski et al. [19]. They calculated a number of one and two-point correlation functions in order to describe short and long-range correlations between itinerant electrons, as well as between itinerant and localized electrons for various ground states. Calculations have been done analytically and by means of well-controlled numerical procedures. In this paper we use the same method to calculate a momentum distribution of itinerant electrons for physically the most interesting cases. In particular, we examine the periodic phases with period two, three and four as well as the phase separated states that are ground states for small (large) f -electron concentrations.

2 The method

Before showing results for the momentum distribution of itinerant electrons in the one-dimensional Falicov-Kimball model let us briefly summarize the main steps of the calculational method [19]. Since in the spinless version of the Falicov-Kimball model without hybridization the f -electron occupation number $f_i^+ f_i$ of each site i commutes with the Hamiltonian (1), the f -electron occupation number is a good quantum number, taking only two values: $w_i = 1$ or 0 , according to whether or not the site i is occupied by the localized f electron and the Hamiltonian (1) can be written as

$$H = \sum_{ij} t_{ij} d_i^+ d_j + U \sum_i w_i d_i^+ d_i + E_f N_f, \quad (2)$$

where $N_f = \sum_i w_i$ denotes the number of f electrons.

Thus for a given f -electron configuration $w = \{w_1, w_2 \dots w_L\}$ defined on a one-dimensional lattice (of L sites) with periodic boundary conditions, the Hamiltonian (2) is the second-quantized version of the single-particle Hamiltonian $h(w)$. If we denote by $\{|i\rangle\}_{i=1,\dots,L}$ the orthogonal basis of one-electron states, such that d_i^+ creates an

electron in the state $|i\rangle$, then the matrix elements of $h(w)$ in the basis $\{|i\rangle\}_{i=1,\dots,L}$ are defined by

$$H(w) = \sum_{i,j=1}^L \langle i|h(w)|j\rangle d_i^\dagger d_j + E_f N_f, \quad (3)$$

where the non-vanishing matrix elements are given by

$$\langle i|h(w)|i\rangle = U w_i, \quad \langle i|h(w)|j\rangle = -1 \quad \text{if } j = i \pm 1. \quad (4)$$

Let $\{|\nu\rangle\}_{\nu=\nu_1,\dots,\nu_L}$ be the orthonormal basis built out of the eigenstates of $h(w)$ to the eigenvalues λ_ν , such that $\lambda_\nu \leq \lambda_{\nu'}$ if $\nu < \nu'$. Then, the unitary matrix \mathcal{U} , with the following matrix elements $\mathcal{U}_{i\nu}$:

$$\mathcal{U}_{i\nu} = \langle i|\nu\rangle, \quad (5)$$

diagonalizes the matrix of $h(w)$,

$$\sum_{i,j} \mathcal{U}_{\nu j}^\dagger \langle j|h(w)|i\rangle \mathcal{U}_{i\nu'} = \lambda_\nu \delta_{\nu\nu'}. \quad (6)$$

Moreover, the set of operators $\{b_\nu^+, b_\nu\}$, $\nu = \nu_1, \dots, \nu_L$, defined by

$$b_\nu = \sum_{i=1}^L \langle \nu|i\rangle d_i, \quad (7)$$

satisfies the canonical anticommutation relations, and

$$H(w) = \sum_{i,j=1}^L \langle i|h(w)|j\rangle d_i^\dagger d_j + E_f N_f = \sum_{\nu} \lambda_\nu b_\nu^+ b_\nu + E_f N_f. \quad (8)$$

Since,

$$d_i = \sum_{\nu} \langle i|\nu\rangle b_\nu, \quad (9)$$

we can express the momentum distribution function of itinerant electrons

$$n_k = \frac{1}{L} \sum_{j,l} e^{ik(j-l)} \langle d_j^\dagger d_l \rangle \quad (10)$$

in terms of the site-components $\langle i|\nu\rangle$ of the eigenvectors $|\nu\rangle$:

$$n_k = \frac{1}{L} \sum_{j,l} e^{ik(j-l)} \sum_{\nu \leq \nu_F} \langle \nu|j\rangle \langle l|\nu\rangle, \quad (11)$$

where ν_F stands for the label of eigenvectors $|\nu\rangle$, such that there is exactly N_d eigenvectors with $\nu \leq \nu_F$. For some low-period ion configurations the eigenproblem can be solved exactly, while for any other ground-state configurations of interest the numerical exact-diagonalization procedure can be used. In the next section we calculate the momentum distribution of itinerant electrons for three periodic phases with the smallest periods as well as for the phase separated ground states. Such a selection of phases is not accidental. In our previous papers [12, 13, 20] we have shown that just these phases occupy the largest regions in the $(E_f - U)$ ground-state phase diagram of the Falicov-Kimball model. Indeed, for large U there is only one nontrivial ground-state phase (besides the empty or fully occupied phase), and namely the two-period phase $w^{(1)} = \{10 \dots 10\}$, and for intermediate values of U there are only two other relevant phases and namely the three-period phase $w^{(2)} = \{110 \dots 110\}$ and the four-period phase $w^{(3)} = \{1110 \dots 1110\}$. These phases are ground states also for small values of U , but in this region also the phase separated configurations, as well as the periodic phases with larger periods can be the ground states of the Falicov-Kimball model. The periodic phases are insulating, and the phase separated configurations are metallic and thus one can expect fully different behavior of the momentum distribution in these ground states.

3 Results and discussion

As was described above one has to know the site-components $\langle i|\nu\rangle$ of the eigenvectors $|\nu\rangle$ to calculate the momentum distribution of itinerant electrons. In order to calculate $\langle i|\nu\rangle$ for $w^{(1)}$, $w^{(2)}$ and $w^{(3)}$ we have generalized the procedure used by Jedrzejewski et al. [19] for analytical calculations of correlation functions in the two-period phase.

For $w^{(n)}$, $n = 1, 2, 3$ the nonvanishing matrix elements of $h(w^{(n)})$ are given by

$$\langle i|h(w^{(n)})|i+1\rangle = -1, \quad \langle i|h(w^{(n)})|i\rangle = Uw_i^{(n)}. \quad (12)$$

One can easily verify that the matrix of $h(w^{(n)})$ can be rewritten to a block-diagonal form by reordering the original basis $\{|k\rangle\}$, $k = 2\pi l/L$, $l = 0, 1, \dots, L-1$. The new basis for $w^{(n)}$, $n = 1, 2, 3$ that reduces $h(w^{(n)})$ to a block-diagonal form is given by:

$$\begin{aligned} &\{|k\rangle, |k+\pi\rangle\}, & n=1, \\ &\{|k\rangle, |k+2\pi/3\rangle, |k+4\pi/3\rangle\}, & n=2, \\ &\{|k\rangle, |k+\pi/2\rangle, |k+\pi\rangle, |k+3\pi/2\rangle\}, & n=3, \end{aligned} \quad (13)$$

where $k = 2\pi l/L$, $l = 0, 1, \dots, L/(n+1) - 1$.

The diagonal blocks are $n+1 \times n+1$ matrices $[h(w^{(n)})]_k$ that in the corresponding basis given by preceding equation have the form

$$[h(w^{(1)})]_k = \begin{bmatrix} \varepsilon_k + \alpha & -\alpha \\ -\alpha & \varepsilon_{k+\pi} + \alpha \end{bmatrix}, \quad \alpha = \frac{U}{2}. \quad (14)$$

$$[h(w^{(2)})]_k = \begin{bmatrix} \varepsilon_k + 2\alpha & -\alpha & -\alpha \\ -\alpha & \varepsilon_{k+2\pi/3} + 2\alpha & -\alpha \\ -\alpha & -\alpha & \varepsilon_{k+4\pi/3} + 2\alpha \end{bmatrix}, \quad \alpha = \frac{U}{3}. \quad (15)$$

$$[h(w^{(3)})]_k = \begin{bmatrix} \varepsilon_k + 3\alpha & -\alpha & -\alpha & -\alpha \\ -\alpha & \varepsilon_{k+\pi/2} + 3\alpha & -\alpha & -\alpha \\ -\alpha & -\alpha & \varepsilon_{k+\pi} + 3\alpha & -\alpha \\ -\alpha & -\alpha & -\alpha & \varepsilon_{k+3\pi/2} + 3\alpha \end{bmatrix}, \quad \alpha = \frac{U}{4}, \quad (16)$$

where $\varepsilon_k = -2 \cos k$.

Let, $\lambda_\mu^{(n)}(k)$ be eigenvalues of $h(w^{(n)})$, i.e.,

$$[h(w^{(n)})]_k |k\rangle_\mu^{(n)} = \lambda_\mu^{(n)}(k) |k\rangle_\mu^{(n)}, \quad \mu = 1, 2, \dots, n+1. \quad (17)$$

Then the corresponding eigenvectors $|k\rangle_\mu^{(n)}$ can be written as:

$$\begin{aligned} |k\rangle_\mu^{(1)} &= x_\mu^{(1)} |k\rangle + y_\mu^{(1)} |k+\pi\rangle, \\ |k\rangle_\mu^{(2)} &= x_\mu^{(2)} |k\rangle + y_\mu^{(2)} |k+2\pi/3\rangle + z_\mu^{(2)} |k+4\pi/3\rangle, \\ |k\rangle_\mu^{(3)} &= x_\mu^{(3)} |k\rangle + y_\mu^{(3)} |k+\pi/2\rangle + z_\mu^{(3)} |k+\pi\rangle + v_\mu^{(3)} |k+3\pi/2\rangle, \end{aligned} \quad (18)$$

where explicit expressions for coefficients $x_\mu^{(n)}, y_\mu^{(n)}, z_\mu^{(n)}, v_\mu^{(n)}$, $n = 1, 2, 3$ are given in Appendix.

Since we are interested in the half-filled band case $N_d + N_f = L$ (which is the point of the special interest for valence and metal-insulator transitions caused by promotion of electrons from localized f orbitals to the conduction band states) we can restrict our considerations to the lowest N_d eigenvalues $\lambda_1^{(n)}(k)$ and the corresponding eigenvectors $|k\rangle_1^{(n)}$, and set

$$|k\rangle^{(n)} \equiv |k\rangle_1^{(n)}, \quad x^{(n)} \equiv x_1^{(n)}, \quad y^{(n)} \equiv y_1^{(n)}, \quad z^{(n)} \equiv z_1^{(n)}, \quad v^{(n)} \equiv v_1^{(n)}. \quad (19)$$

Then, the site-components $\langle m|k\rangle$ for considered phases $w^{(n)}$, $n = 1, 2, 3$ read

$$\begin{aligned} \langle m|k\rangle^{(1)} &= \frac{1}{\sqrt{L}} \left(x^{(1)} e^{ikm} + y^{(1)} e^{i(k+\pi)m} \right), \\ \langle m|k\rangle^{(2)} &= \frac{1}{\sqrt{L}} \left(x^{(2)} e^{ikm} + y^{(2)} e^{i(k+2\pi/3)m} + z^{(2)} e^{i(k+4\pi/3)m} \right), \\ \langle m|k\rangle^{(3)} &= \frac{1}{\sqrt{L}} \left(x^{(3)} e^{ikm} + y^{(3)} e^{i(k+\pi/2)m} + z^{(3)} e^{i(k+\pi)m} + v^{(3)} e^{i(k+3\pi/2)m} \right). \end{aligned} \quad (20)$$

Substituting these expressions into (11) and doing some tedious algebra one obtains the final expression for the momentum distribution of itinerant electrons

$$n_k^{(i)} = |x^{(i)}|^2, \quad i = 1, 2, 3. \quad (21)$$

Using this expression (and corresponding expressions from Appendix) one can plot the momentum distribution of itinerant electrons in the particular phase as a function of k for different values of the Coulomb interaction U . For the two-period phase $w^{(1)}$ the results obtained are displayed in Fig. 1. It is seen that for all examined U the momentum distribution is a smooth function of k . There is no sign of any discontinuity at the Fermi surface $k = k_F = \pi/2$ (the non-Fermi liquid behavior) as well as no sign of singular behavior at $k = k_F$ (the non-Luttinger liquid behavior). This can be verified analytically since the expression (21) (for $i = 1$) can be rewritten as

$$n_k^{(1)} = \frac{1}{2} \left(1 - \frac{\varepsilon_k}{\sqrt{\varepsilon_k^2 + (\frac{U}{2})^2}} \right). \quad (22)$$

Obviously, there is no discontinuity as well as singular behavior at k_F for finite U . Near k_F , $n_k^{(1)}$ behaves like

$$n_k^{(1)} = \frac{1}{2} \left(1 - \frac{k - \pi/2}{\sqrt{(k - \pi/2)^2 + U^2}} \right), \quad (23)$$

what corresponds exactly to the behavior of the Tomonoga-Luttinger fermions coupled by $2k_F$ potential [21]. This potential gives rise to a gap in the energy band spectrum of the Tomonoga-Luttinger fermions, and the appearance of this gap results in the smooth behavior of the momentum distribution. We believe that the same mechanism (the existence of a gap in the charge excitation spectrum at half-filling) is responsible for a smooth behavior of the momentum distribution of the Falicov-Kimball model. The same behavior at half-filling exhibits also the Hubbard model that has a gap in the charge excitation spectrum at $n_\uparrow = n_\downarrow = \frac{1}{2}$, but not for any other density. Since the Falicov-Kimball model can be considered as an approximation to the full Hubbard model in which one part of electrons (say with spin down is immobile), it could be interesting to compare our solution (22) with known results for the momentum distribution of the Hubbard model.

The analytical results for the momentum distribution n_k^H in the Hubbard model are known in the strong coupling limit where the first two terms of the perturbation expansion read [21]

$$n_k^H = \frac{1}{2} \left(1 - \frac{4 \ln 2}{U} \varepsilon_k \right). \quad (24)$$

Comparing this result with the strong coupling expansion of (22)

$$n_k^H = \frac{1}{2} \left(1 - \frac{2}{U} \varepsilon_k \right), \quad (25)$$

one finds that the Falicov-Kimball model (in spite of the above mentioned simplification) contains still much of physics of the full Hubbard model at half-filling. This result is not surprising since for both models there is the antiferromagnetic long-range order in the ground state for $n_d = n_f = n_\uparrow = n_\downarrow = \frac{1}{2}$. Since this ground state persists for all Coulomb interactions $U > 0$ (for both the Hubbard and Falicov-Kimball model) one could expect a good accordance of results also for intermediate and weak interactions. For arbitrary U there is only an approximate (an antiferromagnetic Hartree-Fock) solution for n_k^H in the full Hubbard model [22], that has precisely the same form as our solution for the Falicov-Kimball model.

Outside the half-filling, the momentum distribution behaves, however fully differently in the Falicov-Kimball and Hubbard model. While n_k in the Hubbard model [23] exhibits the power-low singularity at $k = k_F$ for $n_\uparrow = n_\downarrow \neq \frac{1}{2}$ (even for $U \rightarrow \infty$), n_k in the Falicov-Kimball model remains still a continuous function of k for all finite Coulomb interactions. The situation for $n_d = \frac{1}{3}$ (the phase $w^{(2)}$) is displayed in Fig. 2. A continuous character of $n_k^{(2)}$ is obvious for all finite Coulomb interactions U , and increasing U only smears $n_k^{(2)}$. In accordance with the Hubbard model an unusual behavior of the momentum distribution is observed near $n_k = 3k_F$ and U small. However, while the momentum distribution has a weak singularity at $k = 3k_F$ in the Hubbard model [23], it has a local maximum in the Falicov-Kimball model at this point. The similar behavior is observed also for $n_d = \frac{1}{4}$ (see Fig. 3). Again there is a continuous change of $n_k^{(3)}$ at $k = k_F$, with no sign of any discontinuity or singular behavior for finite U . Also an unusual behavior of $n_k^{(3)}$ (a local maximum) is observed at $k = 3k_F$.

To reveal the origin of this unusual behavior we have performed the lowest order perturbation calculations of $n_k^{(i)}$, $i=1,2,3$ in terms of U . A straightforward application of the perturbation procedure [23] yields the following expression for the momentum distribution of itinerant electrons in the Falicov-Kimball model (up to the second

order):

$$n_k^{(l)} = U^2 \sum_{k'} \frac{|V_{k,k'}^{(l)}|^2}{(\varepsilon_k - \varepsilon_{k'})^2} n_{k'}^{(0)}, \quad \text{for } |k| > k_F, \quad (l = 1, 2, 3), \quad (26)$$

where

$$V_{k,k'}^{(l)} = \frac{1}{L} \sum_j e^{i(k-k')R_j} w_j^{(l)} \quad (27)$$

and $n_k^{(0)}$ is the Fermi distribution function of noninteracting electrons.

For the periodic phases $w^{(l)}$ ($l=1,2,3$) the matrix elements $V_{k,k'}^{(l)}$ can be directly calculated and the off-diagonal elements, that enter to Eq. (26), are given by

$$V_{k,k'}^{(l)} = \begin{cases} -\frac{1}{l+1}, & \text{for } k' = k \pm 2nk_F, \quad n = 1, 2 \dots l, \\ 0, & \text{otherwise.} \end{cases} \quad (28)$$

Substituting this expression into Eq. (26) one obtains the final expression for $n_k^{(l)}$

$$n_k^{(l)} = \frac{1}{(l+1)^2} \frac{U^2}{(\varepsilon_k - \varepsilon_{k-2nk_F})^2}, \quad (29)$$

for $k_F(1 + 2(n-1)) < k < k_F(1 + 2n)$.

Analysing this expression one can find that $n_k^{(l)}$ changes its behavior at points $k = 3k_F, 5k_F, 7k_F, \dots$ and this change can produce the local maxima at some points. Indeed, we have found that the second order perturbation theory can describe the local maximum at $k = 3k_F$ for $n_d = \frac{1}{3}$. This is illustrated in Fig. 4 where the momentum distribution (exact as well as perturbation results) is displayed for the periodic phases with the period three, four and six. It is clear that this unusual behavior of the momentum distribution at $k = 3k_F, 5k_F, 7k_F \dots$ is caused by the periodic arrangement of the localized f electrons, which results in a very simple form of off-diagonal matrix elements $V_{k,k'}^{(l)}$. It is interesting that a similar unusual behavior of the momentum distribution at $k = 3k_F, 5k_F, 7k_F \dots$ has been observed (predicted) also in the Hubbard model, however in this case it was assigned to a pair (multipairs) of electron-hole excitations [23].

Finally, let us briefly discuss the case of phase separation. It is well-known [13] that the ground states of the Falicov-Kimball model for sufficiently small Coulomb interactions ($U < 1$) and sufficiently small ($n_d < 1/4$) or large ($3/4 < n_d < 1$) d -electron concentrations are the phase separated configurations, i.e., configurations in which one-half of lattice is fully empty or fully occupied by f -electrons. Such configurations are metallic and we expect fully different behavior of the momentum distribution of itinerant electrons in this phase. Unfortunately, the phase separated configurations are not periodic and thus we cannot proceed in the analytic calculations as in the preceding cases, however, the numerical procedure is still possible. To calculate n_k numerically in the phase separated region (U and n_d small) we need to know exactly the ground-state configuration w^{ps} for selected U and n_d . In general, it is very difficult to find the ground-state configuration for arbitrary U and n_d from the phase separated region, however, it is possible to solve this task for some special values of U and n_d . For example, exhaustive small-cluster exact-diagonalization studies that we have performed in our previous paper [13] for the Falicov-Kimball model in the weak-coupling limit showed that the ground-state configuration of the model for $U = 0.6$ and $n_d = 1/8$ is of the type $w^{ps} = \{111100\dots111100111\dots111\}$. The momentum distribution n_k^{ps} for this configuration (calculated numerically using the procedure described in the preceding section) is displayed in Fig. 5a. As we conjectured the momentum distribution of itinerant electrons behaves fully differently in the metallic phase. It seems that there is a discontinuity (or a singular behavior) in n_k^{ps} at some critical value of $k = k_0 < k_F$. To determine exactly which type of behavior realizes near k_0 we have calculated the finite-size discontinuity $\Delta = n_{k_0 + \frac{2\pi}{L}}^{ps} - n_{k_0 - \frac{2\pi}{L}}^{ps}$ as a function of $1/L$. The results obtained are plotted in Fig. 5b and they clearly show that there is a discontinuity at $k = k_0$. This shows on the Fermi liquid behaviour of itinerant electrons (or some part of them) in the phase separated (metallic) state. To verify this conjecture we have calculated separately

contributions to n_k^{ps} from different parts of a lattice. Since the configuration w^{ps} can be formally considered as a mixture of two phases $w^a = \{111100 \dots 111100\}$ and $w^b = \{111 \dots 111\}$ it is natural to divide the lattice into two parts a and b and to rewrite the summations in Eq. (11) as follows

$$\begin{aligned} n_k^{ps} &= \frac{1}{L} \sum_{j,l} e^{ik(j-l)} \sum_{\nu \leq \nu_F} \langle \nu | j \rangle \langle l | \nu \rangle = \sum_{j,l} \Omega_{j,l} = n_k^a + n_k^{ab} + n_k^{ba} + n_k^b \\ &= \sum_{j \in a, l \in a} \Omega_{j,l} + \sum_{j \in a, l \in b} \Omega_{j,l} + \sum_{j \in b, l \in a} \Omega_{j,l} + \sum_{j \in b, l \in b} \Omega_{j,l}. \end{aligned} \quad (30)$$

The momentum dependence of single contributions n_k^a , n_k^{ab} , n_k^{ba} and n_k^b is plotted in Fig. 6a for two values of L . It is seen that with increasing L the contribution $n_k^{ab} + n_k^{ba}$ goes to zero and thus in the thermodynamic limit $L \rightarrow \infty$ only n_k^a and n_k^b remain finite. The first contribution n_k^a exhibits the same behavior as the momentum distribution in the periodic (insulating) phases $w^{(1)}$, $w^{(2)}$ and $w^{(3)}$. There is no sign of any discontinuity or singular behavior at $k = k_F$. This result is expected since also the phase w^a is periodic. In contrary to this case the second contribution n_k^b exhibits an unexpected behavior of the Fermi liquid type with discontinuity at some critical momentum $k = k_0 = 0.1\pi$ that does not coincides however with the Fermi surface momentum $k_F = \frac{N_d}{L}\pi = 0.125\pi$. Such a behavior as well as the meaning of k_0 can be easily explained within the formalism described above (a mixture of two phases). Let N_d^b be the number of itinerant electrons in the phase w^b . It can be calculated directly from the expression for n_k (Eq. (11)) putting $j = l$ and taking the sum only over the lattice sites from w^b , i.e,

$$N_d^b = \sum_{j \in b} \sum_{\nu \leq \nu_F} \langle \nu | j \rangle \langle j | \nu \rangle. \quad (31)$$

In Fig. 6b we plotted the quantity $k_F^b = \frac{N_d^b}{L^b}\pi$, that represents the Fermi surface of itinerant electrons in w^b , as a function of $1/L$ ($L^b = 5L/8$ denotes the size of w^b phase). It is seen that k_F^b goes to k_0 for $L \rightarrow \infty$ what provides a clear physical

interpretation for k_0 . According to these results the itinerant electrons in the phase w^b behaves like the Fermi liquid with a discontinuity at $k_F^b = \frac{N_d^b}{L^b}\pi = k_0$.

In summary, the momentum distribution n_k of itinerant electrons in the one-dimensional Falicov-Kimball model has been calculated for various ground-state phases. In particular, we have examined the periodic phases with period two, three and four (that are ground-states for all Coulomb interactions) as well as the phase separated states (that are ground states for small Coulomb interactions). We have found that for all periodic phases examined the momentum distribution is a smooth function of k with no sign of any discontinuity or singular behavior at the Fermi surface $k = k_F$. An unusual behavior of n_k (a local maximum) is found at $k = 3k_F$ for electron concentrations outside half-filling. For the phase separated ground states the momentum distribution n_k exhibits discontinuity at $k = k_0 < k_F$. This behavior has been interpreted in terms of a Fermi liquid.

Acknowledgements

This work was supported by the Science and Technology Assistance Agency under Grant APVT-51-021602. Numerical results were obtained using the PC-Farm of the Slovak Academy of Sciences.

4 Appendix

Here we give the explicit expressions for coefficients $x_\mu^{(n)}, y_\mu^{(n)}, z_\mu^{(n)}, v_\mu^{(n)}$ from (18) and the explicit expressions for eigenvalues $\lambda_\mu^{(n)}(k)$ of $h(w^{(n)})$, ($n = 1, 2, 3$):

$$\begin{aligned} x_\mu^{(1)} &= \frac{1-b_\mu^{(1)}}{1-a_\mu^{(1)}} g_\mu^{(1)}, & y_\mu^{(1)} &= g_\mu^{(1)}, \\ g_\mu^{(1)} &= \left\{ 1 + \left(\frac{1-b_\mu^{(1)}}{1-a_\mu^{(1)}} \right)^2 \right\}^{-\frac{1}{2}}, \end{aligned} \tag{32}$$

$$\begin{aligned}
x_\mu^{(2)} &= \frac{1-c_\mu^{(2)}}{1-a_\mu^{(2)}} g_\mu^{(2)}, & y_\mu^{(2)} &= \frac{1-c_\mu^{(2)}}{1-b_\mu^{(2)}} g_\mu^{(2)}, & z_\mu^{(2)} &= g_\mu^{(2)}, \\
g_\mu^{(2)} &= \left\{ 1 + \left(\frac{1-c_\mu^{(2)}}{1-a_\mu^{(2)}} \right)^2 + \left(\frac{1-c_\mu^{(2)}}{1-b_\mu^{(2)}} \right)^2 \right\}^{-\frac{1}{2}},
\end{aligned} \tag{33}$$

$$\begin{aligned}
x_\mu^{(3)} &= \frac{1-d_\mu^{(3)}}{1-a_\mu^{(3)}} g_\mu^{(3)}, & y_\mu^{(3)} &= \frac{1-d_\mu^{(3)}}{1-b_\mu^{(3)}} g_\mu^{(3)}, & z_\mu^{(3)} &= \frac{1-d_\mu^{(3)}}{1-c_\mu^{(3)}} g_\mu^{(3)}, & v_\mu^{(3)} &= g_\mu^{(3)}, \\
g_\mu^{(3)} &= \left\{ 1 + \left(\frac{1-d_\mu^{(3)}}{1-a_\mu^{(3)}} \right)^2 + \left(\frac{1-d_\mu^{(3)}}{1-b_\mu^{(3)}} \right)^2 + \left(\frac{1-d_\mu^{(3)}}{1-c_\mu^{(3)}} \right)^2 \right\}^{-\frac{1}{2}},
\end{aligned} \tag{34}$$

where

$$\begin{aligned}
a_\mu^{(1)}(k) &= -\frac{2}{U} \varepsilon_k - 1 + \frac{2}{U} \lambda_\mu^{(1)}(k), \\
b_\mu^{(1)}(k) &= a_\mu^{(1)}(k + \pi),
\end{aligned} \tag{35}$$

$$\begin{aligned}
a_\mu^{(2)}(k) &= -\frac{3}{U} \varepsilon_k - 2 + \frac{3}{U} \lambda_\mu^{(2)}(k), \\
b_\mu^{(2)}(k) &= a_\mu^{(2)}(k + 2\pi/3), & c_\mu^{(2)}(k) &= a_\mu^{(2)}(k + 4\pi/3),
\end{aligned} \tag{36}$$

$$\begin{aligned}
a_\mu^{(3)}(k) &= -\frac{4}{U} \varepsilon_k - 3 + \frac{4}{U} \lambda_\mu^{(3)}(k), \\
b_\mu^{(3)}(k) &= a_\mu^{(3)}(k + \pi/2), & c_\mu^{(3)}(k) &= a_\mu^{(3)}(k + \pi), & d_\mu^{(3)}(k) &= a_\mu^{(3)}(k + 3\pi/2),
\end{aligned} \tag{37}$$

and

$$\begin{aligned}
\lambda_1^{(1)}(k) &= \frac{U}{2} - \sqrt{\left(\frac{U}{2}\right)^2 + \varepsilon_k^2}, \\
\lambda_2^{(1)}(k) &= \frac{U}{2} + \sqrt{\left(\frac{U}{2}\right)^2 + \varepsilon_k^2},
\end{aligned} \tag{38}$$

$$\begin{aligned}
\lambda_1^{(2)}(k) &= -2r \cos\left(\frac{\phi}{3}\right) + \frac{2U}{3} \\
\lambda_2^{(2)}(k) &= 2r \cos\left(\frac{\pi}{3} + \frac{\phi}{3}\right) + \frac{2U}{3} \\
\lambda_3^{(2)}(k) &= 2r \cos\left(\frac{\pi}{3} - \frac{\phi}{3}\right) + \frac{2U}{3} \\
q &= \cos(3k) + \left(\frac{U}{3}\right)^3, & r &= \sqrt{\left(\frac{U}{3}\right)^2 + 1}, & \phi &= \arccos\left(\frac{q}{r^3}\right),
\end{aligned} \tag{39}$$

$$\begin{aligned}
\lambda_1^{(3)}(k) &= -\frac{\sqrt{6}}{12} p - \frac{1}{12} (48a - 6q - 288cq^{-1} - 24a^2q^{-1} + 72\sqrt{6}bp^{-1})^{1/2} + \frac{3}{4}U, \\
\lambda_2^{(3)}(k) &= -\frac{\sqrt{6}}{12} p + \frac{1}{12} (48a - 6q - 288cq^{-1} - 24a^2q^{-1} + 72\sqrt{6}bp^{-1})^{1/2} + \frac{3}{4}U, \\
\lambda_3^{(3)}(k) &= \frac{\sqrt{6}}{12} p - \frac{1}{12} (48a - 6q - 288cq^{-1} - 24a^2q^{-1} - 72\sqrt{6}bp^{-1})^{1/2} + \frac{3}{4}U, \\
\lambda_4^{(3)}(k) &= \frac{\sqrt{6}}{12} p + \frac{1}{12} (48a - 6q - 288cq^{-1} - 24a^2q^{-1} - 72\sqrt{6}bp^{-1})^{1/2} + \frac{3}{4}U,
\end{aligned} \tag{40}$$

$$\begin{aligned}
a &= 3U^2/8 + 4, & b &= U^3/8, & c &= U^2/4 - 3U^4/256 - 2\cos(4k) + 2, \\
p &= (4a + q + 48cq^{-1} + 4a^2q^{-1})^{1/2}, \\
q &= (288ac + 108b^2 - 8a^3 + 12s)^{1/3}, \\
s &= (-768c^3 + 384c^2a^2 - 48ca^4 + 432acb^2 + 81b^4 - 12b^2a^3)^{1/2}.
\end{aligned} \tag{41}$$

References

- [1] L.M. Falicov and J.C. Kimball, Phys. Rev. Lett. **22**, 997 (1969).
- [2] D.L. Khomskii, *Quantum Theory of Solids*, edited by I.M. Lifshitz (Mir, Moscow 1982).
- [3] T. Portengen, T. Östreich, L.J. Sham, Phys. Rev. Lett. **76**, 3384 (1996).
- [4] J.K. Freericks and L.M. Falicov, Phys. Rev. B. **41**, 2163 (1990).
- [5] Ch. Gruber, D. Ueltschi and J. Jędrzejewski, J. Stat. Phys. **76**, 125 (1994).
- [6] U. Brandt and R. Schmidt, Z. Phys. B **63**, 45 (1986); **67**, 43 (1987).
- [7] T. Kennedy and E.H. Lieb, Physica **138A**, 320 (1986); E.H. Lieb, *ibid.* **140A**, 240 (1986)
- [8] Ch. Gruber, J. Iwanski, J. Jędrzejewski and P. Lemberger, Phys. Rev. B **41**, 2198 (1994); Ch. Gruber, J. Jędrzejewski and P. Lemberger, J. Stat. Phys. **68**, 913 (1992); T. Kennedy, Rev. Math. Phys. **6**, 901 (1994).
- [9] R. Ramirez, L.M. Falicov and J.C. Kimball, Phys. Rev. B. **2**, 3383 (1970).
- [10] U. Brandt and C. Mielsch, Z. Phys. B **75**, 365 (1989); Z. Phys. B **79**, 295 (1990); Z. Phys. B **82**, 37 (1991); see also V. Janiš, Z Phys. B **83**, 227 (1991); P.G.J. van Dongen and D. Vollhardt, Phys. Rev. Lett. **65**, 1663 (1992); P.G.J. van Dongen, Phys. Rev. B **45**, 2267 (1992); J.K. Freericks, Phys. Rev. B **47**, 9263 (1993); **48**, 14797 (1993).
- [11] P. Farkašovský and I. Batko, J. Phys.: Condens. Matter **5**, 7131 (1992).
- [12] P. Farkašovský, Phys. Rev. B **51**, 1507 (1995).
- [13] P. Farkašovský, Phys. Rev. B **52**, R5463 (1995).

- [14] R. Lyzwa, *Physica A* **192**, 231 (1993).
- [15] P. Lemberger, *J. Phys. A* **25**, 715 (1992).
- [16] Ch. Gruber, J.L. Lebowitz and N. Macris, *Europhys. Lett. A* **21**, 389 (1993);
Phys. Rev. B **48** 4312 (1993).
- [17] J.K. Freericks and V. Zlatic, cond-mat/0301188.
- [18] T. Koma and H. Tasaki, *Phys. Rev. Lett.* **68**, 3248 (1992); N. Macris and J. Ruiz, *J. Stat. Phys.* **75**, 1179 (1994); A. Messenger, *Physica A* **279**, 408 (2000).
- [19] J. Jedrzejewski, T. Krokhamalskii and O. Derzhko, cond-mat/0211330.
- [20] P. Farkašovský, *Eur. Phys. J. B* **20**, 209 (2001).
- [21] D. Baeriswyl and W. Von der Linden, *Int. J. Mod. Phys B* **5**, 998 (2001).
- [22] T. Ogawa, K. Kanda and T. Matsubara, *Prog. Theor. Phys.* **53**, 614 (1975).
- [23] M. Ogata, H. Shiba, *Phys. Rev. B* **41**, 2326 (1990).

Figure Captions

Fig. 1. The momentum distribution of the one dimensional Falicov-Kimball model calculated for $n_d = \frac{1}{2}$ and several different values of U .

Fig. 2. (a) The momentum distribution of the one dimensional Falicov-Kimball model calculated for $n_d = \frac{1}{3}$ and several different values of U . (b) The weak-coupling results for the momentum distribution on the enlarged scale.

Fig. 3. (a) The momentum distribution n_k of the one dimensional Falicov-Kimball model calculated for $n_d = \frac{1}{4}$ and several different values of U . (b) The weak-coupling results for the momentum distribution on the enlarged scale.

Fig. 4. (a) The lowest-order perturbation results for the momentum distribution of the Falicov-Kimball model calculated for three different d -electron concentrations. (b) A comparison of exact and perturbation results obtained for $U = 0.1$ and two different d -electron concentrations.

Fig. 5. (a) The momentum distribution n_k^{ps} of the one dimensional Falicov-Kimball model calculated numerically for $n_d = \frac{1}{8}$, $U = 0.6$ and $L = 3200$ sites. (b) The finite-size discontinuity $\Delta = n_{k_0 + \frac{2\pi}{L}}^{ps} - n_{k_0 - \frac{2\pi}{L}}^{ps}$ as a function of $1/L$.

Fig. 6. (a) Contributions to the momentum distribution n_k^{ps} of the one dimensional Falicov-Kimball model at $n_d = \frac{1}{8}$ from different parts of lattice ($U = 0.6$ and $L = 3200$). (b) $k_F^b = \frac{N_d^b}{L^b} \pi$ as a function of $1/L$.

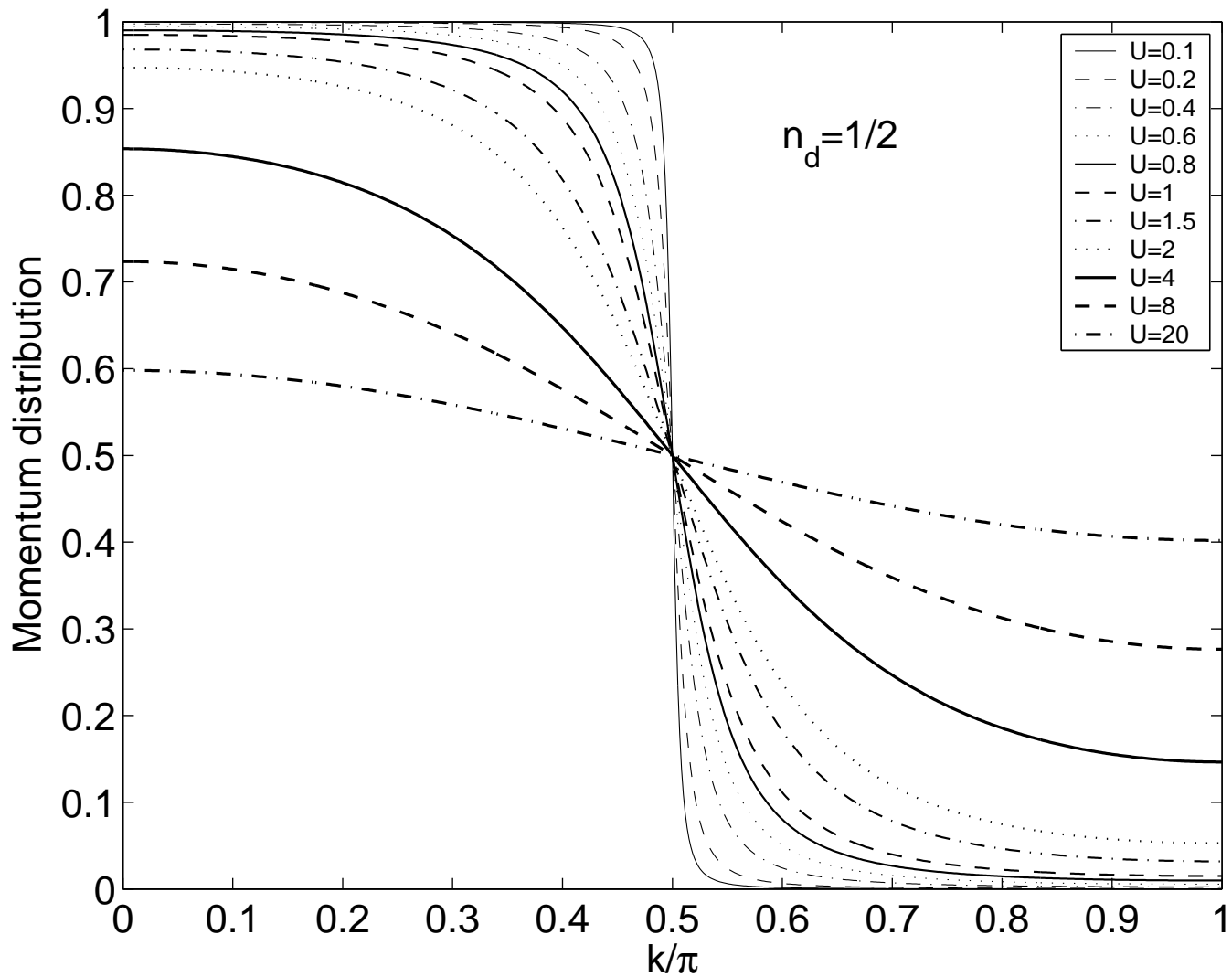


Figure 1:

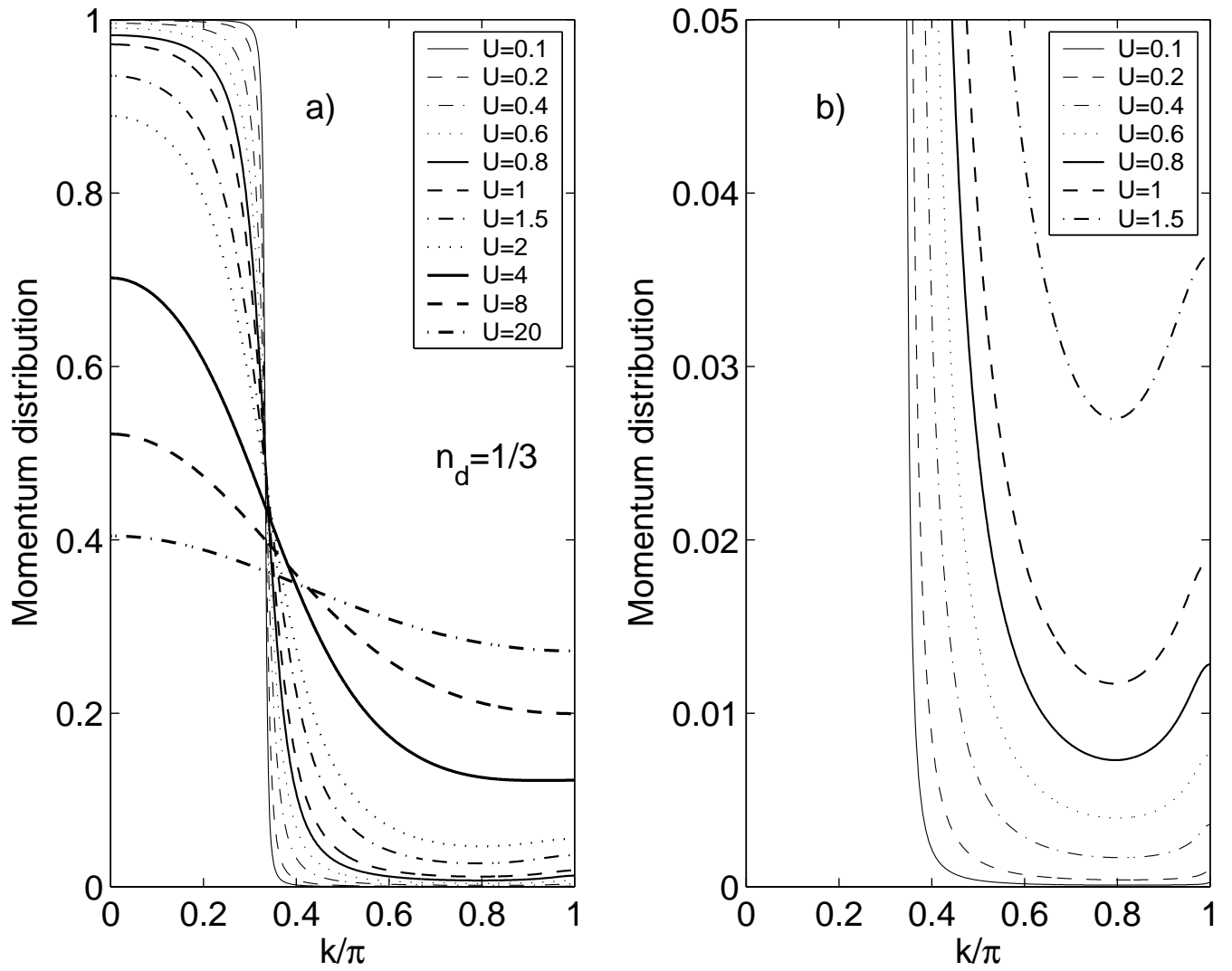


Figure 2:

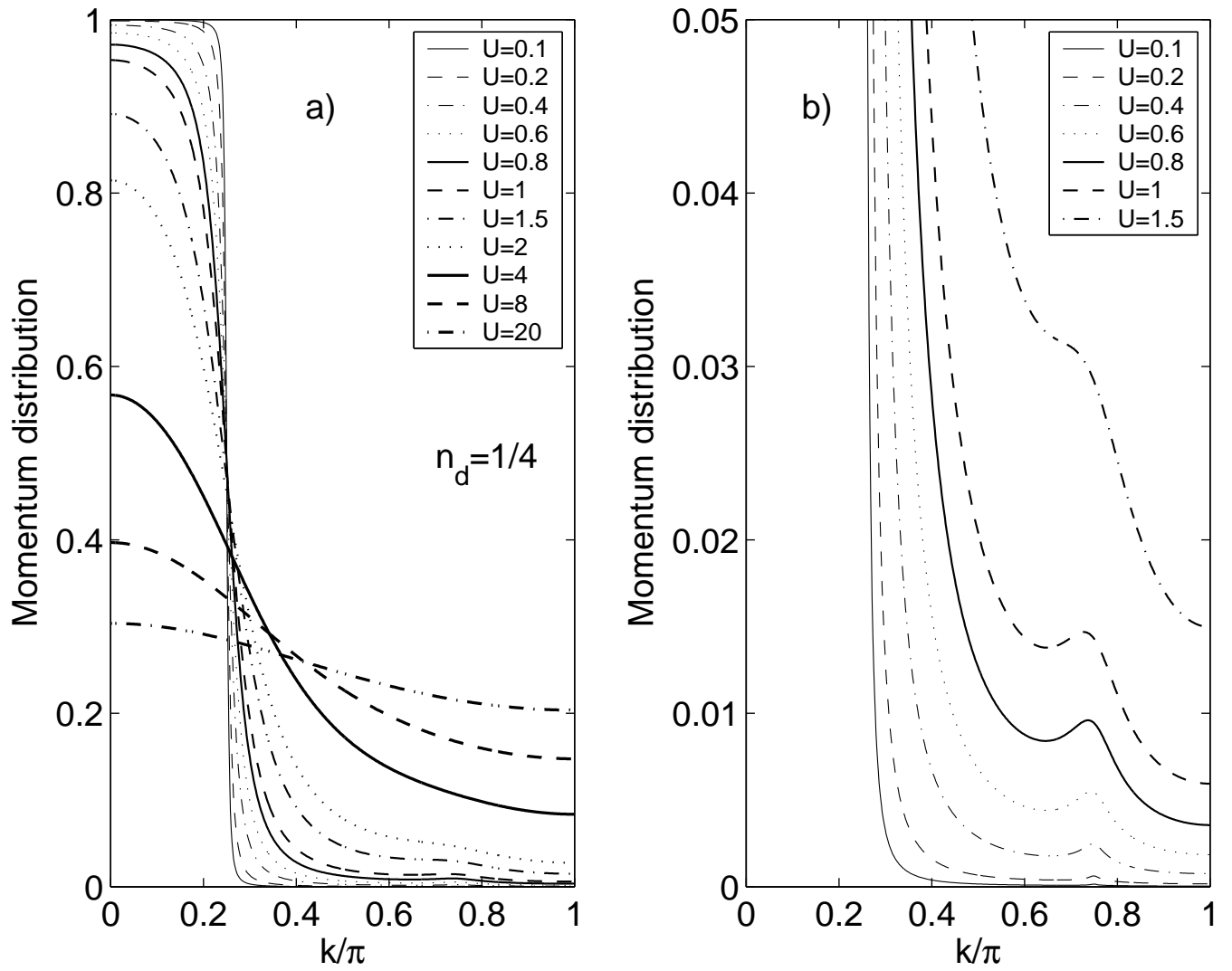


Figure 3:

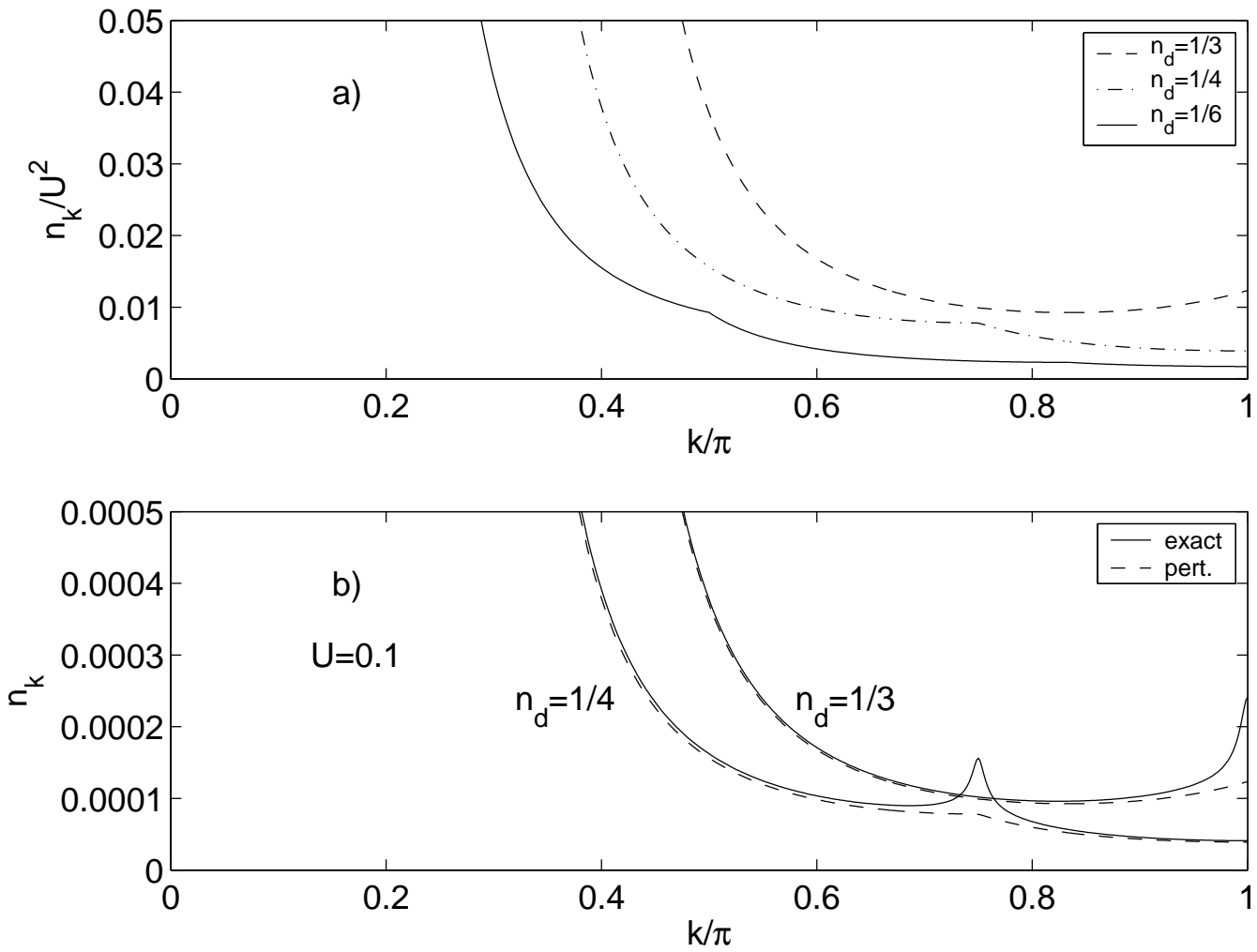


Figure 4:

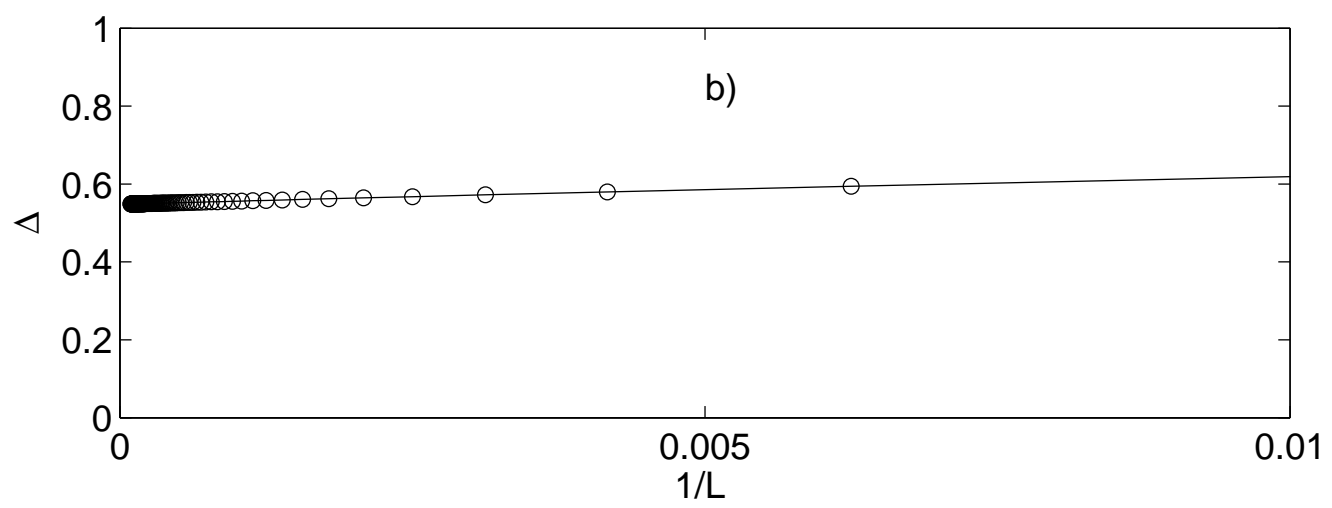
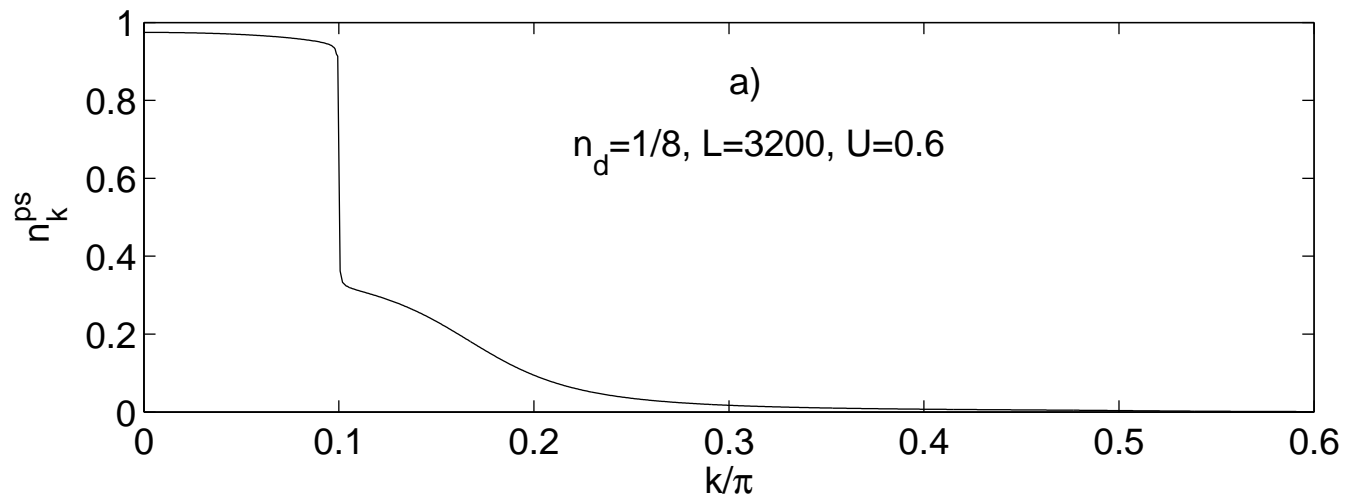


Figure 5:

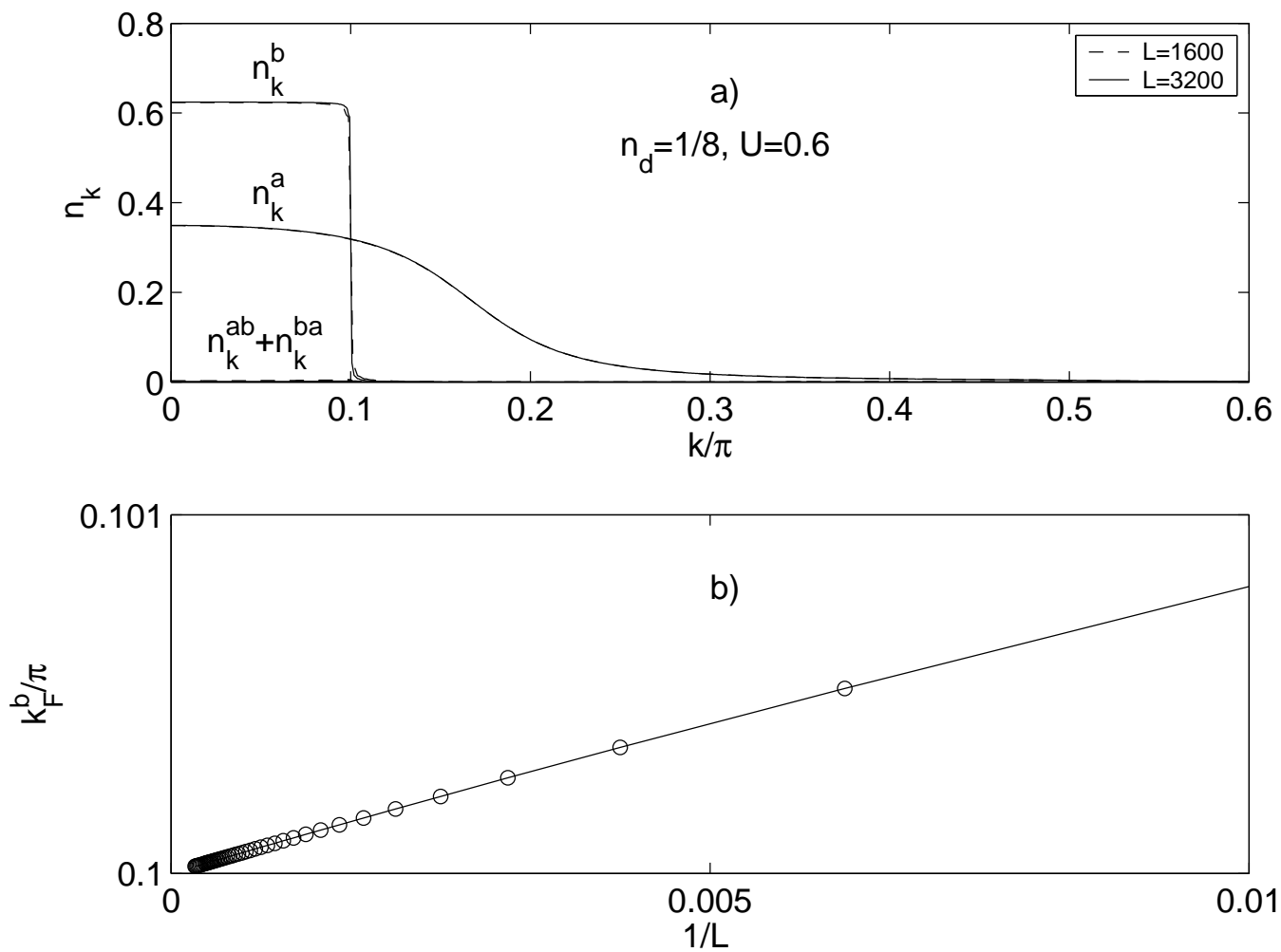


Figure 6: